Isotopic equilibria in aqueous clusters at low temperatures: Insights from the MB-pol many-body potential

Pablo E. Videla,[1,a)] Peter J. Rossky,[2] and Daniel Laria[1,3,b)]
[1]*Departamento de Química Inorgánica Analítica y Química-Física e INQUIMAE, Facultad de Ciencias Exactas y Naturales, Universidad de Buenos Aires, Ciudad Universitaria, Pabellón II, 1428 Buenos Aires, Argentina*
[2]*Department of Chemistry, Rice University, Houston, Texas 77005-1892, USA*
[3]*Departamento de Física de la Materia Condensada, Comisión Nacional de Energía Atómica, Avenida Libertador 8250, 1429 Buenos Aires, Argentina*

(Received 13 December 2017; accepted 6 February 2018; published online 23 February 2018)

By combining path-integrals molecular dynamics simulations with the accurate MB-pol potential energy surface, we investigate the role of alternative potential models on isotopic fractionation ratios between H and D atoms at dangling positions in water clusters at low temperatures. Our results show clear stabilizations of the lighter isotope at dangling sites, characterized by free energy differences ΔG that become comparable to or larger than k_BT for temperatures below ~75 K. The comparison between these results to those previously reported using the empirical q-TIP4P/F water model [P. E. Videla *et al.*, J. Phys. Chem. Lett. **5**, 2375 (2014)] reveals that the latter Hamiltonian overestimates the H stabilization by ~25%. Moreover, predictions from the MB-pol model are in much better agreement with measured results reported for similar isotope equilibria at ice surfaces. The dissection of the quantum kinetic energies into orthogonal directions shows that the dominant differences between the two models are to be found in the anharmonic characteristics of the potential energy surfaces along OH bond directions involved in hydrogen bonds. *Published by AIP Publishing.*
https://doi.org/10.1063/1.5019377

Nuclear quantum effects have deep impacts on a wide variety of thermodynamic properties of hydrogen-bonded substances, water being a paradigmatic example. By now, it is well established that the consideration of zero point energy (ZPE) and tunneling effects is essential to achieve accurate descriptions of the hydrogen bond network of aqueous systems,[1–10] even in thermal regimes as high as those prevailing at ambient conditions. Modifications in many equilibrium thermodynamic quantities upon isotopic substitution represent clear manifestations of these quantum effects, contrasting sharply with classical expectations, in which such differences would be absent. In recent times, many analyses dealing with isotopic equilibria have been carried out from experimental and theoretical perspectives. For example, a series of studies has sought to understand the characteristics of the isotope fractionation ratio of hydrogen (H) and deuterium (D) between liquid water and its vapor phase along the coexistence curve.[11–13] In a related context, H/D isotopic translocations between dangling and connective positions at ice surfaces[14] and at liquid/vapor interfaces[15,16] have also been investigated by a combination of surface-sensitive spectroscopies and computer simulations.

The consideration of aqueous clusters opens new and interesting possibilities to explore the extent of nuclear quantum effects due to two key characteristics prevailing in these systems. First, these aggregates are usually generated from adiabatic expansions at cryogenic temperatures of the order of or below ~100 K,[17–20] a thermal regime where one should expect that the quantum nature of the light nuclei should manifest in a more transparent fashion. Further, the presence of a free surface involving a sizeable fraction of the cluster constituents generates spatial inhomogeneities, giving rise to position dependent H/D isotope equilibria which, in turn, can be monitored by size-selective, spectroscopic techniques.[21]

In a recent article, we presented a path integral molecular dynamics (PIMD) analysis[22] of equilibria associated with the interchange of H and D atoms, from connective (hydrogen bonded) to dangling sites, in different water clusters.[23] In that study, we adopted a Hamiltonian based on the empirical q-TIP4P/F potential energy surface (PES),[24] originally tailored to reproduce experimental (therefore, fully quantum) information of liquid water at ambient conditions. This Hamiltonian includes non-harmonic contributions in the intramolecular stretching interactions, a key element that has proved to be essential to adequately describe isotopic equilibria in aqueous systems.[12] Under these circumstances, it is interesting to inquire about the quality of the conclusions derived from our previous study, when contrasted to a new set of results obtained with a more sophisticated Hamiltonian model. One such model is the many-body MB-pol potential energy surface (PES) recently developed by the Paesani's group.[25–29] This model and parametrization yields highly accurate results for many water properties along a wide variety of thermodynamic states, spanning from low temperature clusters up to

[a)]Current address: Department of Chemistry, Yale University, New Haven, CT 06520-8107, USA.
[b)]Electronic mail: dhlaria@cnea.gov.ar

liquid water at ambient conditions. In addition, the model is very computationally efficient, so it can be implemented in molecular dynamics runs that harvest adequate statistics at still reasonable computational costs. The latter is a significant difference compared to other accurate water models.[30]

In order to retain appropriate control of the connectivity pattern of the clusters under examination, we found it useful to first examine isotopic equilibria in the S_4, solid-like conformer of the $N_w = 8$, water octamer.[23,31] This cluster comprises alternations of single-donor-double-acceptor (SDDA) and double-donor-single-acceptor (DDSA) water molecules, localized at the vertices of a nominally cubic structure [see Fig. 1(a)]. Along a typical simulation run, this arrangement can be preserved for several tens of nanoseconds up to temperatures of the order of ∼175 K beyond which the above-mentioned intermolecular connectivity is lost as the cluster transforms into a much more disordered moiety.[32–34]

The first step in our analysis will be the consideration of the following interconversion process accessible to SDDA molecules

$$H_cOD_d \rightarrow D_cOH_d, \tag{1}$$

where the subscript "d" ("c") denotes a dangling (connective) H atom in a tagged SDDA molecule. The free energy difference, ΔG, associated with the latter equilibrium can be calculated using a standard thermodynamic integration scheme,[35] namely,

$$\Delta G = \int_{m_H}^{m_D} \frac{\langle T_{\mu_d} \rangle - \langle T_{\mu_c} \rangle}{\mu} d\mu, \tag{2}$$

where $\langle T_{\mu_i} \rangle$ represents the average quantum kinetic energy of an isotope of mass μ at position i (i = d, c) which, within the PIMD formalism, can be computed using a virial estimator.[36] Technical details concerning the implementation of the simulation runs are provided as the supplementary material.

In Fig. 2(a), we present results for the temperature dependence of ΔG for Eq. (2) for the water octamer using the MB-pol PES (open circles). The negative values of the free energy difference along the entire range of temperatures investigated reveal a clear propensity of H atoms to occupy dangling

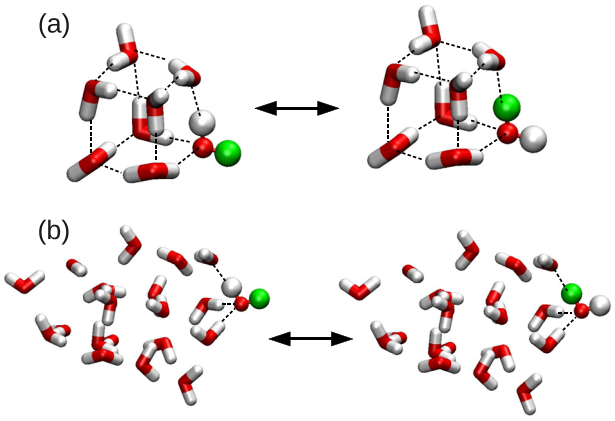

FIG. 1. Isotopic exchange reaction shown in Eq. (1) for two different cluster sizes: (a) water octamer and (b) the 21-mer. For clarity, the water molecule undergoing the mass transformation is distinguished by a "ball and stick" representation. Red, white, and green color represent oxygen, hydrogen, and deuterium atoms, respectively.

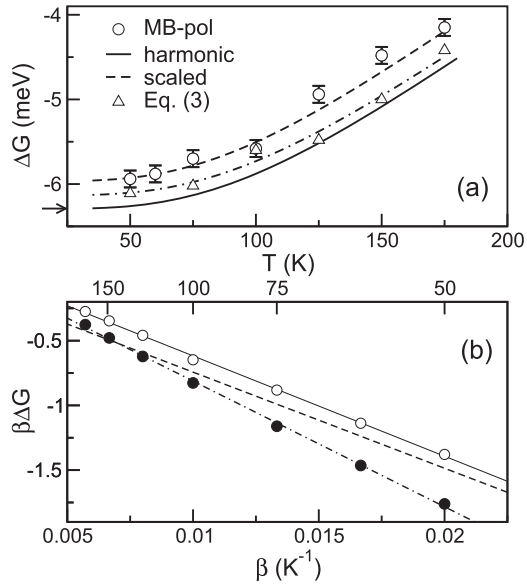

FIG. 2. (a): Temperature dependence of free energy differences. The dot-dashed curve represent a guide to the eye for results obtained from Eq. (3). The arrow at the lower y-axis indicates the harmonic estimate of the ZPE of the MB-pol Hamiltonian (see the text). (b): van't Hoff plots for isotopic exchange equilibrium in the water octamer, for the MB-pol (open circles) and q-TIP4P/F potential (black circles). Solid and dotted-dashed lines represent linear fits of the former results, respectively. Also shown are results from Ref. 14 for isotopic equilibria at ice surfaces (dashed line).

positions, contrasted to D atoms. The extent of this H-stabilization is temperature dependent, becoming more pronounced, the lower the temperature considered, but at a decreasing rate as the vibrational ground states increasingly dominate the result. In Fig. 2(a), we have also included two additional sets of results. The first one corresponds to those computed within the so-called harmonic approximation (solid line), in which quantum free energies at inverse temperatures β were computed as sums of contributions from $3 \times N_w - 6$ uncoupled harmonic oscillators, with non-zero frequencies, calculated at the global minimum of the MB-pol PES of the water octamer (see the supplementary material). The second set (open triangles) was computed from the approximation proposed by Ceriotti and Markland,[37] assuming that the average quantum kinetic energies that appear in the integrand of Eq. (2) scale as $\mu^{-1/2}$ along the $m_H \rightarrow m_D$ mass integration interval, yielding

$$\Delta G \sim 2\left[1 - (m_H/m_D)^{1/2}\right](\langle T_{H_d} \rangle - \langle T_{H_c} \rangle). \tag{3}$$

One appealing feature of the last expression is that it allows for a direct interpretation of the resulting values of ΔG in terms of differences between kinetic energies exclusively of H atoms, at connecting and dangling positions. Within the path integral (PI) formalism, and invoking elementary quantum arguments, one can move a step forward and establish an even more tangible geometrical description of ΔG, based on modifications in the spatial extent of the corresponding isomorphic polymers describing the light isotopes at the above-mentioned sites.

The results of Fig. 2(a) reveal that the two approximations mentioned above exhibit similar qualitative characteristics:

flattening at the lowest temperatures indicating ground state dominance, followed by gradual reductions of the magnitude of ΔG during a thermal interval spanning from ~75 K until the transition to disorder. At low temperatures, the harmonic curve for ΔG extrapolates to the corresponding estimate of the harmonic zero point energy (ZPE) of the MB-pol Hamiltonian (E_0 = −6.29 meV) whereas, for the other two sets, anharmonic contributions shift the ZPE estimates ~0.3 meV higher. Moreover, the low temperature energy gaps between the different sets of results remain practically constant over the whole temperature interval investigated. The results from Eq. (3) are the intermediate between the other two sets since Ceriotti's approximation retains anharmonic ingredients arising from the correct PI evaluation of the average kinetic energies. Interestingly, though, one can partially account for these anharmonic effects within the simpler harmonic description by implementing the common mapping procedure involving a uniform rescaling of the frequencies by a factor of ~0.95 (dashed curve).[38] We remark that similar observations were reported in the calculation of free energy differences between the cage and prism conformers of the water hexamer $[H_2O]_6$.[39]

One can gauge the magnitude of the free energy differences from a different perspective based on the van't Hoff-like plots that are depicted in Fig. 2(b). Note that, as the temperature falls below ~75 K, the magnitude of the MB-pol results (open circles) becomes comparable or higher than k_BT. In other words, at these thermal conditions, the probability of finding H atoms at dangling versus connective positions is already quantum-mechanically enhanced by a factor close to ~3, beyond the direct statistical result based on the consideration of global stoichiometry. Interestingly, the magnitude of this quantum increment in the H-propensity is comparable to the one reported by Devlin[14] at the surfaces of mesoscopic ice clusters, i.e., ~4 at 70 K. For the sake of comparison, note that these enhancements are, at least, one order of magnitude more marked than those observed between dangling and connective OH bonds at macroscopic liquid-vapor interfaces at ambient conditions, which account for only ~10% increments.[15]

Exploiting the observed linear-like dependence of the results, it is also possible to estimate enthalpic differences between the two conformers. A linear fit of the MB-pol results (solid line) yields $\Delta H_{\mathrm{MB-pol}}$ = 6.7 meV, a value which also compares favorably well with the one reported by Devlin, from IR signals at the surfaces of ice nanoclusters at different temperatures, ΔH_{IR} = 6.4 ± 0.1 meV [shown as dashed line in Fig. 2(b)].[14] Note, however, that Devlin's values for ΔG show consistent shifts towards more negative values with respect to MB-pol results, which look slightly more accentuated at higher temperatures. In fact, Devlin's results extrapolate to the $\beta\Delta G$ = 0 classical results linearly as β approaches zero, while the MB-pol must be non-linear. As a rationalization of such discrepancies, one could invoke modifications in the magnitude of the fluctuations of the O···H–O, hydrogen bonds co-linearity and in the amplitude of the librational motions that would prevail at the cluster surfaces comprising a variety of amorphous structures,[14,40,41] contraposed to what is observed in the much simpler structure of the water octamer. These differences would manifest in a more clear fashion as the temperature increases.

Results computed with the q-TIP4P/F Hamiltonian appear in Fig. 2(b) as filled black circles.[42] Compared to those obtained with the MB-pol force field, the empirical model systematically underestimates the values of $\beta\Delta G$. Moreover, the discrepancies become more marked, the lower the temperature. In this case, the linear fit of this new set yields $\Delta H_{\mathrm{q-TIP4P/F}}$ = 8.4 meV (dotted-dashed line), which exceeds the experimental value reported for ice by about a ~30%.

To explore the causes of the differences between results from the two model potentials, we found it convenient to perform the decomposition proposed in Refs. 12 and 15; this consists of expressing ΔG as a sum of orthogonal projections along three relevant orientations: (i) the first corresponds to the direction parallel to the O–H covalent bond vector (hereafter referred to as OH), (ii) the second corresponds to the in-plane (IP) direction that is perpendicular to the OH vector, and (iii) the third corresponds to the out-of-plane (OOP) direction, perpendicular to the plane of the water molecule. In Table I, we present results for such decomposition for both sets of results for T = 50 K. As previously pointed out, results from both Hamiltonian models show that the values of ΔG are the results of delicate interplays between competing quantum projections:[12] (i) the OH contribution is positive, favoring the localization of H atoms at connective positions; (ii) the other two perpendicular projections favor the opposite, i.e., D_cOH_d, configurations. As a corollary, along OH bond directions, the H atoms should exhibit larger spatial dispersion at connecting positions, compared to dangling ones, whereas the opposite trend should be observed along the other two orthogonal directions.[31] In addition to these general trends, the results listed in Table I also reveal that, while the results for the perpendicular decompositions look practically identical for the two models, there is a ~50% increment in the MB-pol, OH projection with respect to the original q-TIP4P/F result.

An analysis based on the expression of Eq. (3) is useful to rationalize these differences. Note that the magnitude of ΔG depends on $\langle T_{H_d}\rangle - \langle T_{H_c}\rangle$ which, in turn, is controlled by the characteristics of the local topologies of the potential energy surfaces at connecting and dangling positions. The crudest way to characterize these topologies involves the examination of their local curvatures. In Table II, we list results for effective frequencies associated with intramolecular OH_i (i = d, c) bonds of a tagged SDDA water molecule. These values correspond to energy differences between the ground and first excited states of potential energy curves obtained by stretching the corresponding OH_i distances, keeping the positions of the rest of the particles fixed at the global minimum energy (see

TABLE I. Decomposition of $\beta\Delta G$ into different components for both model potentials at T = 50 K.[a]

Model	OH	IP	OOP	Total
MB-pol	1.43(3)	−0.96(3)	−1.83(3)	−1.38(3)
q-TIP4P/F	1.08(3)	−0.98(3)	−1.84(3)	−1.74(3)

[a]Uncertainties in the last figure are indicated in parenthesis.

TABLE II. Effective frequencies of OH bonds in the water octamer.[a]

	ω_d	ω_c	$\Delta\omega$
MB-pol	3754	3115	639
q-TIP4P/F	3730	3282	448
Expt.[b]	3723	3066	657

[a]Frequencies in cm^{-1}.
[b]From Ref. 43.

the supplementary material for additional details). The data shown in Table II reveal that these OH frequencies at dangling positions for the two models, ω_d, merely differ by ~25 cm^{-1}; by contrast, the difference observed at connective positions is ~7 times larger. Moreover, the connection between the OH stretching anharmonicities and the parallel free energies can be made more transparent by considering the values of $\Delta\omega = \omega_d - \omega_c$, listed in the last column of Table II. A simple calculation shows that $\Delta\omega^{MB-pol}/\Delta\omega^{q-TIP4P/F} = 1.4$, a value that agrees reasonably well with the ratio of the projections parallel to the OH bonds, namely: $\Delta G_{OH}^{MB-pol}/\Delta G_{OH}^{q-TIP4P/F} = 1.3$.

For the sake of comparison, in the last row of Table II, we have also included experimental values for frequencies extracted from the vibrational spectrum of $[H_2O]_8$, corresponding to the stretching motions localized in SDDA molecules.[43] While the two theoretical predictions for ω_d are still comparable with the experimental one, there is a clear improvement in the quality of the MB-pol prediction for ω_c, which exceeds the experimental value by only ~50 cm^{-1}. We remark that a blue-shift of the order of ~200 cm^{-1} in the position of the latter peak was the major source of discrepancy between the q-TIP4P/F spectrum of the octamer and the IR signal;[31] as such, this new result would indicate that the adoption of the MB-pol force field would, in principle, lead to a better agreement between theory and experimental results. Unfortunately, our efforts to compute IR spectra from approximations involving quantum time correlation functions—such as the ring-polymer-molecular-dynamics approach[44]—led to highly noisy profiles, revealing the lack of appropriate statistics even for trajectories lasting several hundreds of picoseconds.

We finally explored whether or not our conclusions concerning positional isotopic equilibria in the water octamer would still hold in analyses involving larger clusters with more complex hydrogen bond connectivities. Following the same arguments that guided us in our previous analysis,[23] we focused attention on the solid amorphous clusters of the type $[H_2O]_{21}$. Our choice was the result of a compromise between computational feasibility and the possibility of examining moieties sufficiently large so that they would exhibit intermolecular connectivities more akin to the ones prevailing in macroscopic condensed phases. Roughly speaking, these clusters can be portrayed in terms of ovoidal structures, normally presenting ~8–10 dangling molecules randomly distributed at the surface [see Fig. 1(b)]. Additional details concerning the preparation of these larger clusters can be found in Ref. 23. Results for $\beta\Delta G$ at two different temperatures for the two cluster sizes are listed in Table III, where one can observe a practically perfect correspondence between the entries in columns 2 and 3, suggesting an adequate transferability of the

TABLE III. $\beta\Delta G$ for $[H_2O]_{N_w}$.[a]

T (K)	$N_w = 8$	$N_w = 21$
100	–0.66(2)	–0.67(3)
125	–0.46(2)	–0.50(3)

[a]Uncertainties in the last figure are indicated in parenthesis.

octamer results to larger solid-like aggregates and, at the same time, supporting the generality of our previous conclusions.[23] In this respect, the characteristics of the two Hamiltonians are comparable.

Summarizing, we have reexamined the characteristics of positional isotopic equilibria in aqueous clusters at cryogenic temperatures, by combining path integral molecular dynamics simulations with the recently developed and highly accurate MB-pol PES. In the water octamer, these new results confirm a clear stabilization of the D_cOH_d articulation motif, relative to the D_dOH_c alternative. The analysis of the magnitude of these effects, reflected by the values of ΔG, shows a steady increment in the quantum mechanical enhancement of this propensity at lower temperatures, attaining values close to ~3 at temperatures of the order of 75 K. Compared to previous results computed using the empirical q-TIP4P/F model, the new set of values are in better agreement with direct information extracted from the magnitude of the stretching peaks of IR spectra of water at ice surfaces. In addition, data obtained for the non-fluid $[H_2O]_{21}$ cluster indicate that our conclusions concerning the magnitude of the stabilization and its corresponding temperature dependence in the water octamer are also valid for larger and solid-like moieties that exhibit a much more complex intermolecular connectivity.

By dissecting the global results for ΔG along orthogonal projections, we demonstrated that the differences between the results from the two Hamiltonians are dominated by the difference in the potential along OH bonds at connecting positions. These differences are clearly registered in the corresponding frequencies along those directions in SDDA molecules. Moreover, the modifications observed in these frequencies should also appear as a quantitative improvement in the level of agreement in the positions of the low frequency peak of the stretching band between the simulated spectrum and direct experimental signals of the water octamer.

See supplementary material for a detailed description of technical aspects related to simulation and computational procedures.

D.L. is a staff member of CONICET-Argentina. P.J.R. acknowledges the support of the U.S. National Science Foundation (No. CHE-1641076). The research work of D.L. is partially funded by CONICET-Argentina (PIP 112-20110100464). The authors are grateful to Francesco Paesani for providing results ahead of publication and for helpful discussions and comments on an earlier version of this manuscript.

[1]R. A. Kuharski and P. J. Rossky, Chem. Phys. Lett. **103**, 357 (1984).
[2]A. Wallqvist and B. J. Berne, Chem. Phys. Lett. **117**, 214 (1985).
[3]B. J. Berne and D. Thirumalai, Annu. Rev. Phys. Chem. **37**, 401 (1986).
[4]H. A. Stern and B. J. Berne, J. Chem. Phys. **115**, 7622 (2001).

[5]B. Chen, I. Ivanov, M. L. Klein, and M. Parrinello, Phys. Rev. Lett. **91**, 215503 (2003).
[6]T. F. Miller III and D. E. Manolopoulos, J. Chem. Phys. **123**, 154504 (2005).
[7]J. A. Morrone and R. Car, Phys. Rev. Lett. **101**, 017801 (2008).
[8]F. Paesani and G. A. Voth, J. Phys. Chem. B **113**, 5702 (2009).
[9]F. Paesani, S. S. Xantheas, and G. A. Voth, J. Phys. Chem. B **113**, 13118 (2009).
[10]M. Ceriotti, J. Cuny, M. Parrinello, and D. E. Manolopoulos, Proc. Natl. Acad. Sci. U. S. A. **110**, 15591 (2013).
[11]J. Horita and D. J. Wesolowski, Geochim. Cosmochim. Acta **58**, 3425 (1994).
[12]T. E. Markland and B. J. Berne, Proc. Natl. Acad. Sci. U. S. A. **109**, 7988 (2012).
[13]L. Wang, M. Ceriotti, and T. E. Markland, J. Chem. Phys. **141**, 104502 (2014).
[14]J. P. Devlin, J. Chem. Phys. **112**, 5527 (2000).
[15]J. Liu, R. S. Andino, C. M. Miller, X. Chen, D. M. Wilkins, M. Ceriotti, and D. E. Manolopoulos, J. Phys. Chem. C **117**, 2944 (2013).
[16]Y. Nagata, R. E. Pool, E. H. G. Backus, and M. Bonn, Phys. Rev. Lett. **109**, 226101 (2012).
[17]P. Ayotte and M. A. Johnson, J. Chem. Phys. **106**, 811 (1997).
[18]J. R. Verlet, A. E. Bragg, A. Kammrath, O. Cheshnovsky, and D. M. Neumark, Science **307**, 93 (2005).
[19]A. Kammrath, J. R. Verlet, G. B. Griffin, and D. M. Neumark, J. Chem. Phys. **125**, 076101 (2006).
[20]J. R. Verlet, A. E. Bragg, A. Kammrath, O. Cheshnovsky, and D. M. Neumark, Science **310**, 1769 (2005).
[21]U. Buck and F. Huisken, Chem. Rev. **100**, 3863 (2000).
[22]M. E. Tuckerman, *Statistical Mechanics: Theory and Molecular Simulation* (Oxford University Press, 2010), Chap. 10.
[23]P. E. Videla, P. J. Rossky, and D. Laria, J. Phys. Chem. Lett. **5**, 2375 (2014).
[24]S. Habershon, T. E. Markland, and D. E. Manolopoulos, J. Chem. Phys. **131**, 024501 (2009).
[25]V. Babin, C. Leforestier, and F. Paesani, J. Chem. Theory Comput. **9**, 5395 (2013).
[26]V. Babin, G. R. Medders, and F. Paesani, J. Chem. Theory Comput. **10**, 1599 (2014).
[27]V. Babin, G. R. Medders, and F. Paesani, J. Chem. Theory Comput. **10**, 2906 (2014).
[28]G. R. Medders and F. Paesani, J. Chem. Theory Comput. **11**, 1145 (2015).
[29]G. R. Medders, A. W. Gotz, M. A. Morales, P. Bajaj, and F. Paesani, J. Chem. Phys. **143**, 104102 (2015).
[30]Y. Wang, X. Huang, B. C. Shepler, B. J. Braams, and J. M. Bowman, J. Chem. Phys. **134**, 94509 (2011).
[31]P. E. Videla, P. J. Rossky, and D. Laria, J. Chem. Phys. **139**, 174315 (2013).
[32]E. Asare, A. R. Musah, E. Curotto, D. L. Freeman, and J. D. Doll, J. Chem. Phys. **131**, 184508 (2009).
[33]P. Nigra, M. A. Carignano, and S. Kais, J. Chem. Phys. **115**, 2621 (2001).
[34]L. F. L. Oliveira, J. Cuny, M. Morinière, L. Dontot, A. Simon, F. Spiegelman, and M. Rapacioli, Phys. Chem. Chem. Phys. **17**, 17079 (2015).
[35]J. Vanicek and W. H. Miller, J. Chem. Phys. **127**, 114309 (2007).
[36]M. F. Herman, J. Bruskin, and B. J. Berne, J. Chem. Phys. **76**, 5150 (1982).
[37]M. Ceriotti and D. E. Markland, J. Chem. Phys. **138**, 14112 (2013).
[38]B. Temelso and G. G. Shields, J. Chem. Theory Comput. **7**, 2804 (2011).
[39]Y. Wang, V. Babin, J. M. Bowman, and F. Paesani, J. Am. Chem. Soc. **134**, 11116 (2012).
[40]B. Rowland, M. Fisher, and J. P. Devlin, J. Chem. Phys. **95**, 1378 (1991).
[41]B. Rowland, N. S. Kadagathur, J. P. Devlin, V. Buch, T. Feldman, and M. J. Wojcik, J. Chem. Phys. **102**, 8328 (1995).
[42]Results for $T = 50$ K and $T = 75$ K differ from those previously reported in Ref. 23 and correspond to new, fully converged runs.
[43]U. Buck, I. Ettischer, M. Melzer, V. Buch, and J. Sadlej, Phys. Rev. Lett. **80**, 2578 (1998).
[44]S. Habershon, D. E. Manolopoulos, T. E. Markland, and T. F. Miller III, Annu. Rev. Phys. Chem. **64**, 387 (2013).